0022-3565/09/3301-162–168$20.00
THE JOURNAL OF PHARMACOLOGY AND EXPERIMENTAL THERAPEUTICS
Copyright © 2009 by The American Society for Pharmacology and Experimental Therapeutics
JPET 330:162–168, 2009

Vol. 330, No. 1
150730/3479788
Printed in U.S.A.

The Journal of PHARMACOLOGY And Experimental Therapeutics

G_i-Dependent Cell Signaling Responses of the Human $P2Y_{14}$ Receptor in Model Cell Systems

Ingrid P. Fricks, Rhonda L. Carter,[1] Eduardo R. Lazarowski, and T. Kendall Harden

Departments of Pharmacology (I.P.F., R.L.C., T.K.H.) and Medicine (E.R.L.) and the Cystic Fibrosis Center (E.R.L.), University of North Carolina School of Medicine, Chapel Hill, North Carolina

Received January 11, 2009; accepted March 31, 2009

ABSTRACT

Eight G protein-coupled receptors comprise the P2Y receptor family of cell signaling proteins. The goal of the current study was to define native cell signaling pathways regulated by the uridine nucleotide sugar-activated $P2Y_{14}$ receptor ($P2Y_{14}$-R). The $P2Y_{14}$-R was stably expressed in human embryonic kidney (HEK) 293 and C6 rat glioma cells by retroviral infection. Nucleotide sugar-dependent $P2Y_{14}$-R activation was examined by measuring inhibition of forskolin-stimulated cAMP accumulation. The effect of $P2Y_{14}$-R activation on mitogen-activated protein kinase signaling also was studied in $P2Y_{14}$-HEK293 cells and in differentiated HL-60 human myeloid leukemia cells. UDP-Glc, UDP-galactose, UDP-glucuronic acid, and UDP-*N*-acetylglucosamine promoted inhibition of forskolin-stimulated cAMP accumulation in $P2Y_{14}$-HEK293 and $P2Y_{14}$-C6 cells, and this signaling effect was abolished by pretreatment of cells with pertussis toxin. Inhibition of cAMP formation by nucleotide sugars also was observed in direct assays of adenylyl cyclase activity in membranes prepared from $P2Y_{14}$-C6 cells. UDP-Glc promoted concentration-dependent and pertussis toxin-sensitive extracellular signal-regulated kinase (ERK) 1/2 phosphorylation in $P2Y_{14}$-HEK293 cells. $P2Y_{14}$-R mRNA was not observed in wild-type HL-60 cells but was readily detected in dimethyl sulfoxide-differentiated cells. Consistent with this observation, no effect of UDP-Glc was observed in wild-type HL-60 cells, but UDP-Glc-promoted pertussis toxin-sensitive activation of ERK1/2 occurred after differentiation. These results illustrate that the human $P2Y_{14}$-R signals through G_i to inhibit adenylyl cyclase, and $P2Y_{14}$-R activation also leads to ERK1/2 activation. This work also identifies two stable $P2Y_{14}$-R-expressing cell lines and differentiated HL-60 cells as model systems for the study of $P2Y_{14}$-R-dependent signal transduction.

The $P2Y_{14}$-R is a seven-transmembrane-spanning G protein-coupled receptor that is activated by UDP-Glc and other UDP sugars (Chambers et al., 2000). $P2Y_{14}$-R mRNA is expressed in stomach, intestine, placental and adipose tissues, lung, heart, and throughout the brain, and in many types of immune cells (Lee et al., 2003; Moore et al., 2003; Skelton et al., 2003; Scrivens and Dickenson, 2006). Consistent with its prominent immune cell expression, the $P2Y_{14}$-R has been implicated in several immune cell functions. Moore et al. (2003) reported that $P2Y_{14}$-R mRNA is up-regulated in several brain regions after immunological challenge of mice with lipopolysaccharide. In addition, UDP-Glc was reported to promote chemotaxis of bone marrow-derived hematopoietic stem cells (Lee et al., 2003).

The $P2Y_{14}$-R is a member of a subgroup of P2Y receptors, which includes the $P2Y_{12}$ and $P2Y_{13}$ receptors thought primarily to activate heterotrimeric G proteins of the G_i family, but a comprehensive understanding of the signal transduction pathways activated by the $P2Y_{14}$-R is not available. Nonetheless, several reports are consistent with the idea that the $P2Y_{14}$-R couples to G_i. For example, Chambers and his colleagues illustrated in their initial study of the cloned human $P2Y_{14}$-R that UDP-Glc promotes pertussis toxin-sensitive binding of radiolabeled GTPγS to membranes prepared from HEK293 cells expressing this receptor. Modest UDP-Glc-promoted inhibition of cAMP accumulation also has been reported for murine T-lymphocytes (Scrivens and Dickenson, 2005), human neutrophils (Scrivens and Dickenson, 2006), and C6 glioma cells (Krzemiński et al., 2008), although the effects were not shown unambiguously to involve the $P2Y_{14}$-R. Other pharmacological studies of the $P2Y_{14}$-R have

This work was supported by the National Institutes of Health National Institute of General Medical Sciences and National Heart, Lung, and Blood Institute [Grants GM38213, HL34322].

[1] Current affiliation: Thomas Jefferson University, School of Pharmacy, Philadelphia, Pennsylvania.

Article, publication date, and citation information can be found at http://jpet.aspetjournals.org.
doi:10.1124/jpet.109.150730.

ABBREVIATIONS: $P2Y_{14}$-R, $P2Y_{14}$ receptor; HEK, human embryonic kidney; MAP, mitogen-activated protein kinase; DMEM, Dulbecco's modified Eagle's medium; FBS, fetal bovine serum; DMSO, dimethyl sulfoxide; IBMX, 3-isobutyl-1-methylxanthine; ERK, extracellular signal-regulated kinase; JNK, c-Jun NH_2-terminal kinase; RT, reverse transcriptase; PCR, polymerase chain reaction; fMLP, formyl-Met-Leu-Phe; PAR, protease-activated receptor; FPR, formyl peptide receptor.

Downloaded from jpet.aspetjournals.org at ASPET Journals on January 20, 2018

relied on coexpression with the promiscuous G protein, $G\alpha_{16}$ (Chambers et al., 2000), or with a chimeric G_q (Moore et al., 2003; Fricks et al., 2008) engineered to couple G_i-activating receptors to activation of phosphoinositide hydrolysis and Ca^{2+} mobilization (Coward et al., 1999).

Studies of the $P2Y_{14}$-R have been limited by inability to detect and quantify receptor expression directly through the use of antibodies or radioligand binding assays and also by the absence of high-affinity, nonhydrolyzable, selective agonists, and competitive antagonists to verify receptor-specific signal transduction. It is critical that we understand the cell signaling processes engaged in response to $P2Y_{14}$-R activation, and with this goal in mind, we generated two different cell lines that stably express the human $P2Y_{14}$-R. Robust $P2Y_{14}$-R-dependent inhibition of adenylyl cyclase was observed in both cell lines, and $P2Y_{14}$-R-dependent MAP kinase signaling was studied in $P2Y_{14}$-HEK293 cells. We also discovered that expression of native $P2Y_{14}$-R is induced during differentiation of HL-60 human myeloid leukemia cells and that UDP-Glc promotes activation of MAP kinase signaling in these cells. The model cell systems reported here should provide useful platforms for investigation of the $P2Y_{14}$-R at the cellular and biochemical level.

Materials and Methods

Cell Culture. HEK293 cells were grown in Dulbecco's modified Eagle's medium (DMEM) supplemented with 10% fetal bovine serum (FBS) at 37°C in a 10% CO_2 environment. C6 rat glioma cells were cultured in DMEM supplemented with 5% FBS in a 5% CO_2 environment. HL-60 cells were maintained in Iscove's medium supplemented with 10% FBS. Differentiation of HL-60 cells was achieved by inclusion of 1.3% DMSO in the culture medium for 5 days (Servant et al., 2000).

$P2Y_{14}$-R Expression. Human $P2Y_{14}$-R cDNA was amplified and ligated into the retroviral expression vector pLXSN as described previously (Wolff et al., 2005). Retrovirus encoding the $P2Y_{14}$-R was produced in PA317 cells according to the method of Johnson et al. (1998) and was used to infect HEK293 cells or C6 glioma cells. Geneticin-resistant cells were selected for 2 weeks in medium containing 0.4 mg/ml G418. Clonal HEK293 cells stably expressing the $hP2Y_{14}$-R were obtained by performing serial dilutions of cells in 96-well plates and growing clonal populations from a single cell under selection medium.

Membrane Preparation. Membranes were prepared as described previously (Smith and Harden, 1985). In brief, $P2Y_{14}$-C6 rat glioma cells were grown on 150-mm dishes until confluent. Cells were washed gently with phosphate-buffered saline and then lysed with ice-cold 1 mM Tris, pH 7.4. Cells were harvested by scraping dishes and homogenized with a glass homogenizer for 10 strokes. Lysates were centrifuged at 40,000*g* for 10 min. Membranes were resuspended in 10 mM Tris, pH 7.4, containing 1 mM EDTA and centrifuged again at 40,000*g* for 10 min. Washed membranes were resuspended in assay buffer (25 mM HEPES, pH 7.4, 5 mM MgCl, 150 mM NaCl, 1 mM EDTA) and used immediately.

cAMP Accumulation. Cells were grown in 24-well plates and incubated with 1 μCi [^{3}H]adenine/well in serum-free DMEM for 2 h before assay. Assays were initiated by the addition of HEPES-buffered, serum-free DMEM containing 200 μM 3-isobutyl-1-methylxanthine (IBMX), with or without drugs, and incubation continued for 12 min at 37°C. Incubations were terminated by aspiration of medium and addition of 450 μl of ice-cold 5% trichloroacetic acid. [^{3}H]cAMP was isolated by sequential Dowex and alumina chromatography (Salomon et al., 1974) and quantified by liquid scintillation counting.

Adenylyl Cyclase Activity. Quantification of adenylyl cyclase activity was carried out according to the procedure described previously (Harden et al., 1982). In brief, assay tubes on ice contained drug or buffer and a reaction mix of assay buffer containing, at final assay concentrations, 0.01 mM [α-^{32}P]ATP (10–15 cpm/pmol), 0.5 mM [^{3}H]cAMP (10,000 cpm/assay), 8 mM creatine phosphate, creatine phosphokinase (6 U/assay), 0.01 mM GTP, 0.2 mM IBMX, 25 mM HEPES, pH 7.5, 5 mM $MgSO_4$, 2 mM EDTA, and 150 mM NaCl. Assays were initiated by the addition of 100 μg of membrane protein, and the incubations were carried out for 12 min at 30°C. The reaction was terminated with addition of 0.85 ml of ice-cold 5% trichloroacetic acid. [^{32}P]cAMP was isolated by sequential Dowex and alumina chromatography and quantified by liquid scintillation counting. Recovery of [^{3}H]cAMP over columns averaged 50 to 60%.

MAP Kinase Activation Assays. HEK293 cells were grown on 12-well plates until 70 to 90% confluent. Cells were serum-starved 24 h before assay. Drugs were added to cells for the indicated times, and the assay was terminated by aspiration of medium. The cells were washed once with phosphate-buffered saline, and Laemmli buffer containing 60 μM dithiothreitol was added to each well. The resultant cell lysates were passed through a 27-gauge needle 10 times, heated to 95°C for 5 min, and proteins were resolved by electrophoresis on a 12.5% polyacrylamide gel. Proteins were transferred to a nitrocellulose membrane, blocked with 5% bovine serum albumin, washed with Tris-buffered saline/Tween 20 (20 mM Tris, pH 7.4, 120 mM NaCl, 0.1% Tween 20), and then incubated with antibody for phospho-ERK1/2, phospho-p38, or phospho-c-Jun NH_2-terminal kinase (JNK), according to the manufacturer's directions. After washing with Tris-buffered saline/Tween 20, membranes were incubated with horseradish peroxidase-conjugated goat-anti-mouse (phospho-ERK1/2, phospho-JNK) or goat-anti-rabbit (phospho-p38) antibody, membranes were washed, incubated with chemiluminescent substrate (Pico West system; Thermo Fisher Scientific, Waltham, MA), and then exposed to film. Membranes were stripped with 200 mM glycine, pH 2.6, for 1 h at 25°C, then reprobed with a primary antibody against total MAP kinase to verify equal loading of lanes. HL-60 cells were serum-starved 24 h before the assay and resuspended in Hanks' balanced salt solution for the assay at a density of 5×10^6 cells/ml, 0.2 ml/assay. Drugs were added for the indicated times, and the cells were lysed by adding 1 volume of Laemmli buffer containing 60 μM dithiothreitol to the cells. Lysates were analyzed as described above.

Reverse Transcriptase-PCR. HL-60 cells were harvested, washed, and lysed in TRIzol reagent (Invitrogen, Carlsbad, CA). Total RNA was isolated by chloroform extraction, and isolation of mRNA was performed using the Oligotex mRNA Mini kit (QIAGEN, Valencia, CA). cDNA was generated using the reverse transcriptase (RT) III SuperMix First-Strand Synthesis kit (Invitrogen). $P2Y_{14}$-R-specific primers (5′-ACTACGCGTCCATCAATTCAA-3′ and 5′-GTTAGTGACATCCTTAACACTCTGGTTGGTGAGAAT-3′) were used in the PCR reactions, and conditions were as follows: 95°C, 30 s; 55°C, 30 s; and 72°C, 1 min, for 38 cycles. PCR products were analyzed by 2% agarose gel electrophoresis and visualized by ethidium bromide staining. Negative controls for each sample were performed without reverse transcriptase added to the reaction.

Data Analysis. EC_{50} values were determined using Prism software (GraphPad Software Inc., San Diego, CA) and are presented as mean ± S.E. Statistical significance was determined by analysis of variance, and $p < 0.02$ was considered statistically significant. All experiments were repeated at least three times.

Materials. IBMX, creatine phosphate, creatine phosphokinase, forskolin, formyl-Met-Leu-Phe (fMLP), and GTP were purchased from Sigma-Aldrich (St. Louis, MO). UDP-Glc, UDP-galactose, UDP-glucuronic acid, and UDP-*N*-acetylglucosamine were all from Fluka (Buchs, Switzerland), purchased through Sigma-Aldrich. HPLC analysis of the UDP-Glc used in the current experiments revealed >98% purity. ATP was purchased from GE Healthcare (Chalfont St. Giles, UK). Pertussis toxin was purchased from List Biological Laboratories Inc.(Campbell, CA). [^{3}H]Adenine and [^{3}H]cAMP were purchased from American Radiolabeled Chemicals (St. Louis, MO).

Downloaded from jpet.aspetjournals.org at ASPET Journals on January 20, 2018

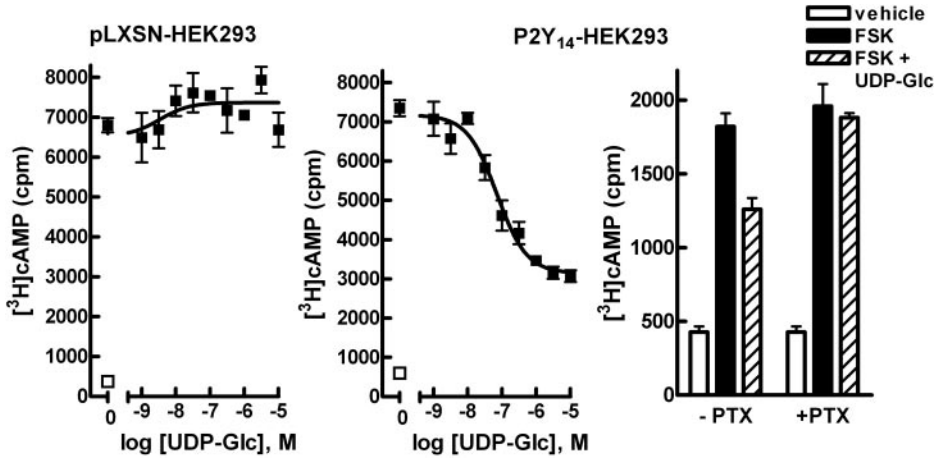

Fig. 1. Concentration-dependent and pertussis toxin-sensitive inhibition of cAMP accumulation promoted by UDP-Glc in $P2Y_{14}$-HEK293 cells. Empty vector-infected (left) or $P2Y_{14}$-R-expressing (middle) cells were labeled with [^{3}H]adenine 18 h before assay. Cells were incubated with 200 μM IBMX in the absence (□) or presence of 30 μM forskolin and the indicated concentrations of UDP-Glc (■) for 12 min before quantification of [^{3}H]cAMP accumulation. $P2Y_{14}$-R-expressing (right) cells were preincubated overnight with 100 ng/ml pertussis toxin, and [^{3}H]cAMP accumulation was measured in the presence of 200 μM IBMX alone (open bars), 200 μM IBMX + 30 μM forskolin (filled bars), or 200 μM IBMX + 30 μM forskolin + 10 μM UDP-Glc (hatched bars). The data shown are presented as mean ± S.E. and are representative of results from three independent experiments.

[α-^{32}P]ATP was purchased from PerkinElmer Life and Analytical Sciences (Waltham, MA). Antibodies for P-ERK1/2, ERK1/2, P-p38, p38, P-JNK, and JNK were purchased from Cell Signaling Technology Inc. (Danvers, MA). All cell culture medium and serum were from Invitrogen. The protease-activated receptor (PAR) agonist peptide SLIGKV was a generous gift from Dr. Joann Trejo. Anisomycin and sorbitol were kind gifts from Dr. Gary Johnson.

Results

UDP Sugars Promote Inhibition of Forskolin-Stimulated cAMP Formation in Cells Stably Expressing the Human $P2Y_{14}$-R. To examine potential regulation of adenylyl cyclase activity downstream of the human $P2Y_{14}$-R, we stably expressed this receptor in HEK293 cells. UDP-Glc promoted concentration-dependent inhibition of forskolin-stimulated accumulation of cAMP in $P2Y_{14}$-R-expressing HEK293 cells. An EC_{50} value of 82 ± 11 nM (n = 3) was observed for UDP-Glc, and the maximal inhibition of forskolin-stimulated cAMP accumulation ranged from 50 to 60% (Fig. 1). In contrast, no effect of UDP-Glc was observed on basal or forskolin-stimulated cAMP accumulation in HEK293 cells infected with vector alone. Preincubation of $P2Y_{14}$-HEK293 cells with pertussis toxin resulted in complete loss of UDP-Glc-dependent inhibition of cAMP accumulation (Fig. 1), indicating that the $P2Y_{14}$-R signals through Gα-subunits of the G_i family.

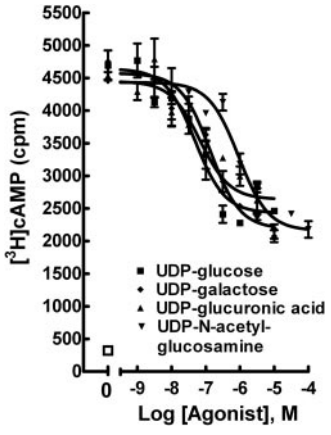

Fig. 2. UDP-galactose, UDP-glucuronic acid, and UDP-*N*-acetylglucosamine inhibit accumulation of cAMP in $P2Y_{14}$-HEK293 cells. [^{3}H]Adenine-labeled $P2Y_{14}$-HEK293 cells were incubated with 200 μM IBMX alone (□) or IBMX with 30 μM forskolin and varying concentrations of UDP-Glc (■), UDP-galactose (♦), UDP-glucuronic acid (▲), or UDP-*N*-acetylglucosamine (▼). Data shown are mean ± S.E. and are representative of results of three independent experiments.

Although UDP-Glc is reported to be a full agonist at the $P2Y_{14}$-R, several studies of the $P2Y_{14}$-R have reported variable effects of other nucleotide sugars (Chambers et al., 2000; Scrivens and Dickenson, 2006). Therefore, we tested the capacity of UDP sugars to activate the $P2Y_{14}$-R in $P2Y_{14}$-HEK293 cells. UDP-galactose, UDP-glucuronic acid, and UDP-*N*-acetylglucosamine all promoted inhibition of cAMP accumulation, and the maximal inhibition observed was similar to that of UDP-Glc. The potencies of UDP-galactose and UDP-glucuronic acid were similar to that of UDP-Glc, whereas UDP-*N*-acetylglucosamine exhibited an approximately 10-fold higher EC_{50} value (Fig. 2; Table 1). Although marked $P2Y_{14}$ receptor-dependent effects on cAMP accumulation were observed in $P2Y_{14}$-HEK293 cells, incubation of these cells with UDP-Glc had no effect on inositol phosphate accumulation (data not shown).

We concluded that it was important to stably express the $P2Y_{14}$-R in several cell backgrounds. Previous studies by our lab and other labs revealed robust inhibition of adenylyl cyclase in C6 rat glioma cells expressing several different G protein-coupled receptors (Schachter et al., 1997; Thomas et al., 2000; Castillo et al., 2007). Therefore, we also infected C6 cells with the recombinant pLXSN virus harboring the $hP2Y_{14}$-R coding sequence. Again, although UDP-Glc had no effect on cAMP accumulation in C6 cells expressing empty vector alone, robust inhibitory effects were observed with UDP-Glc in $P2Y_{14}$-R-expressing C6 cells, with 70 to 80% maximal inhibition of forskolin-stimulated accumulation of cAMP (Fig. 3). An EC_{50} value of 107 ± 68 nM was determined (Table 1). The action of UDP-Glc in $P2Y_{14}$-C6 cells was completely blocked by pretreatment of the cells with pertussis toxin (Fig. 3). The concentration-dependent inhibition of cAMP formation with other UDP sugars also was established, and the EC_{50} values are reported in Table 1.

Effect of UDP-Glc on Adenylyl Cyclase Activity in Membranes from $P2Y_{14}$-R-Expressing C6 Cells. Based on the robust $P2Y_{14}$-R-dependent inhibition of cAMP accumulation observed in C6 glioma cells, we also isolated plasma membrane-enriched fractions to determine whether UDP-Glc- and $P2Y_{14}$-R-dependent inhibition of adenylyl cyclase activity could be observed in a cell-free system. Although no effect of UDP-Glc was observed in membranes from control cells, approximately 50% inhibition of forskolin-stimulated

Downloaded from jpet.aspetjournals.org at ASPET Journals on January 20, 2018

TABLE 1

EC_{50} values for $P2Y_{14}$-R agonists in $P2Y_{14}$-HEK293 and $P2Y_{14}$-C6 cells

[^{3}H]Adenine-labeled cells were incubated with IBMX (200 μM), forskolin (30 μM), and varying concentrations of UDP-glucose, UDP-galactose, UDP-glucuronic acid, or UDP-*N*-acetylglucosamine for 15 min. [^{3}H]cAMP was quantified as described under *Materials and Methods*. EC_{50} values and percentage inhibition were determined with GraphPad Prism software and are presented as mean ± S.E. or percentage inhibition of forskolin-stimulated cAMP accumulation. Results are derived from three independent experiments.

Agonist	$hP2Y_{14}$-HEK293		$hP2Y_{14}$-C6	
	EC_{50} ± S.E.	Maximal Inhibition	EC_{50} ± S.E.	Maximal Inhibition
	nM	%	*nM*	%
UDP-glucose	82 ± 11	51 ± 1	92 ± 51	76 ± 0.5
UDP-galactose	96 ± 29	60 ± 2	240 ± 53	72 ± 8
UDP-glucuronic acid	60 ± 7	55 ± 0.3	108 ± 66	79 ± 1
UDP-*N*-acetylglucosamine	919 ± 205	58 ± 3	225 ± 68	74 ± 8

adenylyl cyclase activity was observed in the presence of 10 μM UDP-Glc in membranes isolated from $P2Y_{14}$-C6 glioma cells (Fig. 4). This UDP-Glc-promoted response did not occur in membranes from $P2Y_{14}$-C6 cells pretreated with pertussis toxin.

MAP Kinase Activation by UDP-Glc in $P2Y_{14}$-HEK293 Cells. Many important biological processes are regulated by MAP kinase signaling pathways. To assess the capacity of the $P2Y_{14}$-R to activate MAP kinase signaling cascades, $P2Y_{14}$-HEK293 cells were treated with UDP-Glc, and cell lysates were analyzed for phosphorylated ERK1/2 by Western blotting. Although no effect was observed in mock-infected cells, UDP-Glc-dependent ERK1/2 phosphorylation occurred in $P2Y_{14}$-HEK293 cells (Fig. 5A).

The time course for UDP-Glc activation of ERK1/2 was compared with that occurring as a consequence of activation of PAR2, which is natively expressed in HEK293 cells (Amadesi et al., 2004; Dai et al., 2007). Incubation of cells with the PAR2 agonist peptide SLIGKV (100 μM) resulted in marked phosphorylation of ERK1/2 within 5 min, but phosphorylation quickly diminished thereafter. In contrast, UDP-Glc-dependent activation of ERK1/2 was not maximal until at least 15 min of incubation and was retained for at least 30 min. The effect of UDP-Glc on ERK1/2 phosphorylation was concentration-dependent (Fig. 5C), and the EC_{50} (30 nM) observed was similar to that obtained in studies of inhibition of cAMP accumulation in these cells. As was observed in the studies of adenylyl cyclase activity, $P2Y_{14}$-R-regulated ERK1/2 phosphorylation was not observed in cells preincubated with pertussis toxin (Fig. 5B).

The capacity of the $P2Y_{14}$-R to activate p38 and JNK also was examined. Although p38 was phosphorylated with a peak response observed within 5 min after treatment of cells with sorbitol, no UDP-Glc-dependent activation of p38 was observed at any time point up to 60 min (Fig. 5D). In contrast to a robust activation observed in the presence of anisomycin, we also observed no effect of UDP-Glc on JNK phosphorylation (Fig. 5D).

Functional $P2Y_{14}$-R Are Endogenously Expressed in Differentiated HL-60 Cells. With the goal of identifying a cell line that natively expresses the $P2Y_{14}$-R, we tested by RT-PCR several candidate cell lines previously reported to express $P2Y_{14}$-R mRNA and other cell lines derived from tissues reported to express this receptor (Chambers et al., 2000; Moore et al., 2003; Skelton et al., 2003). Although no $P2Y_{14}$-R mRNA was detected in undifferentiated HL-60 cells, differentiation of these cells with 1.3% DMSO to a neutro-

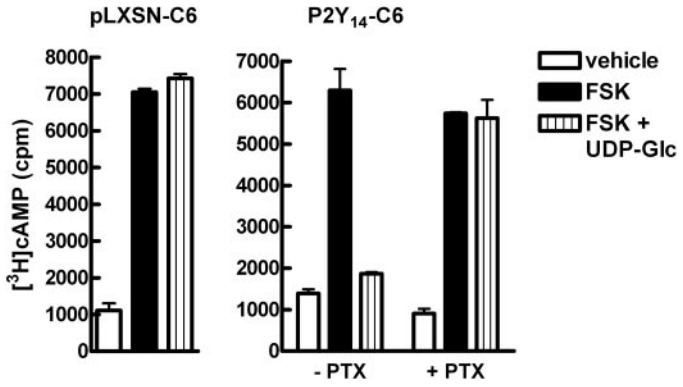

Fig. 3. UDP-Glc promotes pertussis toxin-sensitive inhibition of cAMP accumulation in $P2Y_{14}$-C6 cells. Empty vector-infected (left) C6 rat glioma cells were prelabeled with [^{3}H]adenine and then incubated in the presence of 200 μM IBMX alone (open bar), 200 μM IBMX + 30 μM forskolin (filled bar), or 200 μM IBMX + 30 μM forskolin + 10 μM UDP-Glc (striped bar). $P2Y_{14}$-C6 cells (right) were incubated in the absence or presence of 100 ng/ml pertussis toxin before quantification of [^{3}H]cAMP accumulation in the presence of 200 μM IBMX alone (open bars), 200 μM IBMX + 30 μM forskolin (filled bars), or 200 μM IBMX + 30 μM forskolin + 10 μM UDP-Glc (striped bars). Data shown are presented as mean ± S.E. and are representative of results from three independent experiments.

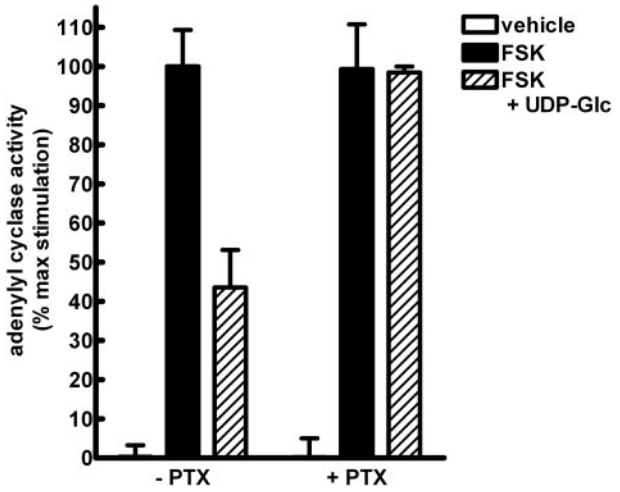

Fig. 4. UDP-Glc-dependent inhibition of adenylyl cyclase by UDP-Glc in membranes from $P2Y_{14}$-C6 cells. Membranes were isolated from $P2Y_{14}$-C6 cells or from cells pretreated with 100 ng/ml pertussis toxin overnight. Membranes were incubated with 200 μM IBMX in the absence (open bars) or presence (filled bars) of 30 μM forskolin or with 200 μM IBMX + 30 μM forskolin + 10 μM UDP-Glc (hatched bars) as described under *Materials and Methods*. [^{32}P]cAMP was isolated by sequential Dowex-alumina chromatography. Data shown are the mean ± S.E. of three independent experiments, plotted as a percentage of maximal forskolin-stimulated enzyme activity.

Downloaded from jpet.aspetjournals.org at ASPET Journals on January 20, 2018

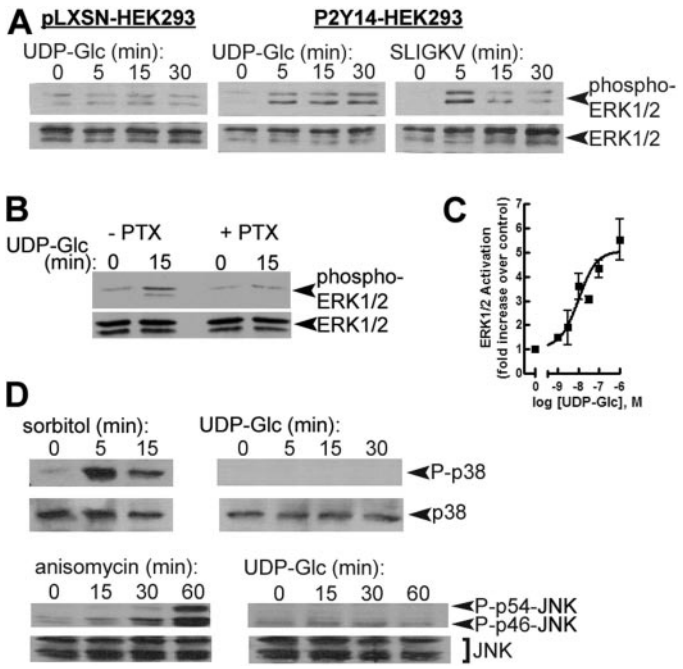

Fig. 5. UDP-Glc-promoted activation of MAP kinase signaling in $P2Y_{14}$-HEK293 cells. A, empty vector or $P2Y_{14}$-R-expressing HEK293 cells were serum-starved for 18 h and then incubated with 100 μM UDP-Glc or 100 μM SLIGKV for the times indicated. Cell lysates were subjected to SDS-polyacrylamide gel electrophoresis, the samples were transferred to nitrocellulose membranes, and the samples were probed with antibodies for phospho-ERK1/2 and total ERK1/2 as described under *Materials and Methods*. Results shown are representative of three individual experiments. B, cells were pretreated in the absence (−PTX) or presence (+PTX) of 100 ng/ml pertussis toxin overnight, then treated with UDP-Glc for 15 min. Results shown are representative of those obtained from three independent experiments. C, cells were incubated with varying concentrations of UDP-Glc for 15 min. Phospho-ERK1/2 and ERK1/2 were quantified using Scion Image software (Scion Corporation, Frederick, MD) and graphed using GraphPad Prism software. Each phospho-ERK1/2 lane was normalized to the corresponding ERK1/2 control and plotted as fold stimulation over control. Data shown are the average ± S.E. of four independent experiments. D, $P2Y_{14}$-HEK293 cells were treated with 0.2 M sorbitol, 0.01 mg/ml anisomycin, or 100 μM UDP-Glc for the indicated times. Phospho-p38, phospho-JNK, total p38, and total JNK were determined as described under *Materials and Methods*.

phil-like cell resulted in a marked increase in expression of $P2Y_{14}$-R mRNA (Fig. 6A).

We also investigated the cell signaling responses discussed above to determine whether functional $P2Y_{14}$-R could be observed in differentiated HL-60 cells. In multiple experiments, 100 μM UDP-Glc exhibited no effect on cAMP accumulation promoted by forskolin, amthamine, an agonist for the Gs-coupled H2 histamine receptor, or forskolin + amthamine (data not shown). Although a formyl peptide receptor (FPR) is natively expressed by HL-60 cells (Boulay et al., 1990; Klinker et al., 1996), we also failed to observe effects of 1 μM fMLP on cAMP accumulation in these cells.

Potential activation of the MAP kinase signaling pathway also was studied in HL-60 cells. Although no effect of UDP-Glc was observed in wild-type cells, time-dependent activation of ERK1/2 by UDP-Glc was observed after differentiation of the cells. This effect was apparent within 5 min and peaked within 30 min (Fig. 6B). In contrast to the time course of the phosphorylation response to UDP-Glc, cells treated with 1 μM fMLP exhibited a robust ERK1/2 activation at 5 min that quickly diminished thereafter (Fig. 6C). Neither

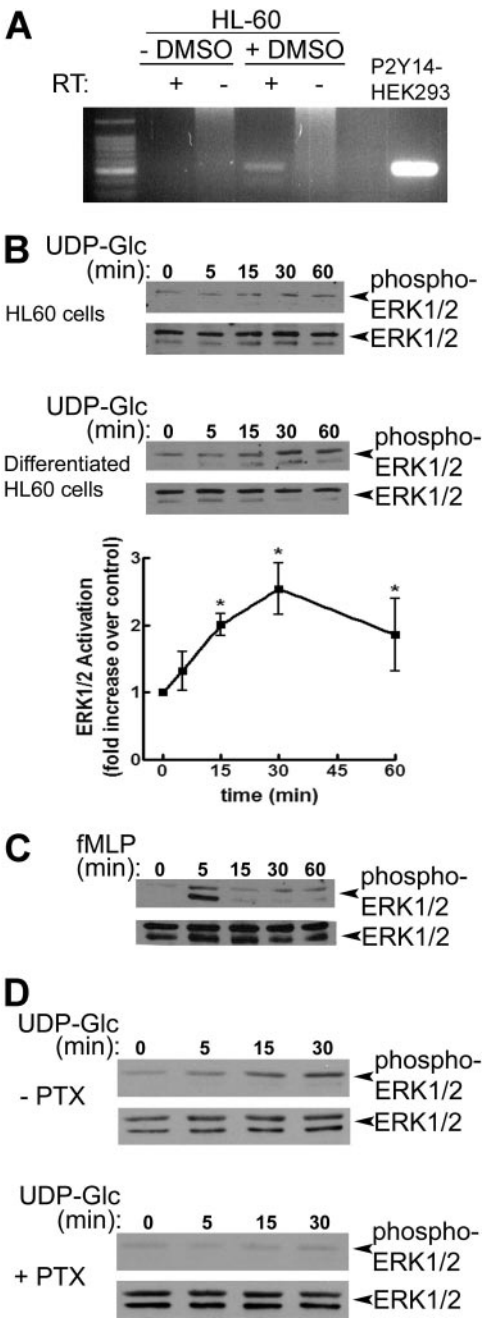

Fig. 6. UDP-Glc-promoted activation of MAP kinase activation in differentiated HL-60 cells. A, RT-PCR of undifferentiated (−DMSO) or differentiated (+DMSO) HL-60 cells in the absence (−) or presence (+) of RT. PCR with $hP2Y_{14}$-R-specific primers was performed as described under *Materials and Methods*. B, wild-type or differentiated (see *Materials and Methods*) HL-60 cells were serum-starved for 18 h before addition of 100 μM UDP-Glc, and incubation was continued for the indicated times. Western blots for phospho-ERK1/2 and ERK1/2 were generated as described under *Materials and Methods*. Phospho-ERK1/2 was quantified using Scion Image software and graphed using GraphPad Prism software. Each phospho-ERK1/2 lane was normalized to the corresponding ERK1/2 control and plotted as -fold stimulation over control. Data shown are the mean ± S.E. of six independent experiments (*, $p < 0.02$). C, serum-starved, differentiated HL-60 cells were incubated with 1 μM formyl-Met-Leu-Phe for the indicated times, and lysates were analyzed as described under *Materials and Methods*. D, differentiated HL-60 cells were treated in the absence (−PTX) or presence (+PTX) of 200 ng/ml pertussis toxin for 4 h before assay. Cells were incubated for the indicated times with 100 μM UDP-Glc and phospho-ERK1/2, and total ERK1/2 was quantified as described under *Materials and Methods*.

Downloaded from jpet.aspetjournals.org at ASPET Journals on January 20, 2018

UDP-Glc- nor fMLP-dependent ERK1/2 activation was observed in cells preincubated with pertussis toxin (Fig. 6D), consistent with the notion that the UDP-Glc-promoted ERK1/2 activation in differentiated HL-60 cells occurs through a mechanism involving G_i in differentiated HL-60 cells.

Discussion

In this report, we demonstrate that the human $P2Y_{14}$-R couples to inhibition of adenylyl cyclase in a pertussis toxin-sensitive manner in HEK293 and C6 cells stably expressing this receptor. This work provides the first unequivocal demonstration of $P2Y_{14}$-R-dependent inhibition of adenylyl cyclase in a membrane preparation. Robust stimulation of MAP kinase signaling also occurs with activation of the $P2Y_{14}$-R. This was the predominant activity observed with native $P2Y_{14}$-R in differentiated HL-60 human myeloid leukemia cells.

UDP-Glc is released from many cell types. This phenomenon was initially demonstrated by Lazarowski et al. (2003), who illustrated both basal and mechanically induced release of UDP-Glc from multiple mammalian cell types. Constitutive release of UDP-Glc also occurs in yeast (Esther et al., 2008). Although the mechanism(s) underlying UDP-Glc release is not well established, calcium-dependent release of UDP-Glc was demonstrated in Calu-3 cells (Kreda et al., 2007), and UDP-Glc release occurred downstream of thrombin receptor-promoted signaling pathways in human astrocytoma 1321N1 cells (Kreda et al., 2008).

UDP sugars in addition to UDP-Glc are predictably present in the extracellular space. UDP-Glc, UDP-galactose, UDP-glucuronic acid, and UDP-*N*-acetylglucosamine all were reported previously as potent agonists of the $P2Y_{14}$-R in test systems that involved coexpression of the receptor with a phospholipase C-activating G protein (Chambers et al., 2000; Freeman et al., 2001). Our results measuring responses of a native signaling pathway also indicate that these four UDP sugars are full agonists and exhibit relatively similar potencies. It remains to be elucidated which one or more of these molecules is the endogenous agonist(s) for the receptor. Indeed, multiple UDP sugars likely are physiological agonists for the $P2Y_{14}$-R, such that the activating ligand may differ according to tissue or cell type.

Our findings that neither UDP-Glc nor fMLP had an effect on cAMP accumulation in differentiated HL-60 cells indicates that activated G_i does not couple to inhibition of adenylyl cyclase in these cells. Perhaps the isoforms of adenylyl cyclase expressed in these cells are not subject to inhibition by G_i, as has been demonstrated for neutrophils (Mahadeo et al., 2007). HL-60 cells gain a neutrophil phenotype upon differentiation and, therefore, are likely to reflect receptor-promoted signaling responses that are characteristic of neutrophils. Receptor-promoted inhibition of adenylyl cyclase has not been unequivocally demonstrated in neutrophils, and we are unaware of studies clearly defining the signaling pathways downstream of G_i-coupled receptors in these cells. A small inhibition of cAMP accumulation was reported to occur upon incubation of neutrophils with UDP-Glc (Scrivens and Dickenson, 2006). However, it is unclear whether this was a $P2Y_{14}$-R-mediated effect.

G_i-coupled GPCR activate MAP kinase signaling, and we illustrate here that UDP-Glc-dependent activation of ERK1/2 occurs in $P2Y_{14}$-HEK293 cells. Although $P2Y_{14}$-R were not detected in undifferentiated HL-60 cells, a message for the $P2Y_{14}$-R was observed upon differentiation of HL-60 cells, and occurrence of UDP-Glc-promoted MAP kinase signaling indicated the presence of functional $P2Y_{14}$-R. RT-PCR analyses previously demonstrated that neutrophils express $P2Y_{14}$-R at the RNA level (Chen et al., 2006). However, $P2Y_{14}$-R were not detected in HL-60 cells, and it is unclear whether differentiated HL-60 cells were examined by these authors.

HL-60 cells have been used as a model of neutrophil-like cells that undergo differentiation-associated morphological and functional changes including up-regulation of chemoattractant receptors and the capacity to chemotax (Hauert et al., 2002). Differentiated HL-60 cells exhibit capacities to generate superoxide, ingest particles, and degranulate with efficiencies similar to that of neutrophils (Newburger et al., 1979). In addition, they have distinct technical advantages over primary cells, such as viability and transfectability. Differentiated HL-60 cells also have been used as a model system for studies of FPR, and consistent with previous observations (Rane et al., 1997; Christophe et al., 2002; Paruch et al., 2006), we observed fMLP-promoted ERK1/2 activation in differentiated HL-60 cells. These findings establish differentiated HL-60 cells as a model system for investigation of biological functions of the $P2Y_{14}$-R.

The duration of $P2Y_{14}$-R-promoted ERK1/2 phosphorylation in HEK293 cells and HL-60 cells was prolonged compared with that of other G protein-coupled receptors. PAR2, which promoted very transient ERK1/2 activation in HEK293 cells, is known to couple to G_i, $G_{12/13}$, and G_q (Fyfe et al., 2005). The fMLP receptor, FPR, has been reported to couple to G_i, but the mechanism linking FPR to ERK1/2 phosphorylation is not clear (Selvatici et al., 2006; Huet et al., 2007; Kam et al., 2007). Therefore, it is possible that the signaling pathway(s) responsible for $P2Y_{14}$-R-promoted MAP kinase signaling differs from that engaged by PAR2 or FPR. We speculate that pertussis toxin-sensitive Gα-subunits are necessary but not sufficient, and additional pathways or regulatory mechanisms are involved in the MAP kinase response downstream of one or more of these receptors. Our studies do not rule out the possibility that the $P2Y_{14}$-R desensitizes at a slower rate than PAR2 in HEK293 cells or FPR in HL-60 cells. Additional studies will be necessary to address questions about the mechanism of $P2Y_{14}$-R-dependent activation of MAP kinase, but its pertussis toxin sensitivity clearly indicates that G_i is an important signaling component in the pathway.

In summary, this work unequivocally demonstrates that the human $P2Y_{14}$-R promotes inhibition of adenylyl cyclase and activation of MAP kinase signaling pathways. Our work also provides several model cell lines for study of $P2Y_{14}$-R signaling and its potential role in neutrophil biology.

Acknowledgments

We thank Matthew Barrett for excellent technical assistance. We also acknowledge helpful discussions with Tiffany Ricks and Lisa Stalheim and Drs. Yixing Zhou, Matthew Cheever, Robert Nicholas, JoAnn Trejo, and Amy Abell.

Downloaded from jpet.aspetjournals.org at ASPET Journals on January 20, 2018

References

Amadesi S, Nie J, Vergnolle N, Cottrell GS, Grady EF, Trevisani M, Manni C, Geppetti P, McRoberts JA, Ennes H, et al. (2004) Protease-activated receptor 2 sensitizes the capsaicin receptor transient receptor potential vanilloid receptor 1 to induce hyperalgesia. *J Neurosci* **24:**4300–4312.

Boulay F, Tardif M, Brouchon L, and Vignais P (1990) The human *N*-formylpeptide receptor: characterization of two cDNA isolates and evidence for a new subfamily of G-protein-coupled receptors. *Biochemistry* **29:**11123–11133.

Castillo CA, Albasanz JL, Fernández M, and Martín M (2007) Endogenous expression of adenosine A1, A2 and A3 receptors in rat C6 glioma cells. *Neurochem Res* **32:**1056–1070.

Chambers JK, Macdonald LE, Sarau HM, Ames RS, Freeman K, Foley JJ, Zhu Y, McLaughlin MM, Murdock P, McMillan L, et al. (2000) A G protein-coupled receptor for UDP-glucose. *J Biol Chem* **275:**10767–10771.

Chen Y, Corriden R, Inoue Y, Yip L, Hashiguchi N, Zinkernagel A, Nizet V, Insel PA, and Junger WG (2006) ATP release guides neutrophil chemotaxis via $P2Y_2$ and A3 receptors. *Science* **314:**1792–1795.

Christophe T, Karlsson A, Rabiet MJ, Boulay F, and Dahlgren C (2002) Phagocyte activation by Trp-Lys-Tyr-Met-Val-Met, acting through FPRL1/LXA4R, is not affected by lipoxin A4. *Scand J Immunol* **56:**470–476.

Coward P, Chan SD, Wada HG, Humphries GM, and Conklin BR (1999) Chimeric G proteins allow a high-throughput signaling assay of G_i-coupled receptors. *Anal Biochem* **270:**242–248.

Dai Y, Wang S, Tominaga M, Yamamoto S, Fukuoka T, Higashi T, Kobayashi K, Obata K, Yamanaka H, and Noguchi K (2007) Sensitization of TRPA1 by PAR2 contributes to the sensation of inflammatory pain. *J Clin Invest* **117:**1979–1987.

Esther CR Jr, Sesma JI, Dohlman HG, Ault AD, Clas ML, Lazarowski ER, and Boucher RC (2008) Similarities between UDP-glucose and adenine nucleotide release in yeast: involvement of the secretory pathway. *Biochemistry* **47:**9269–9278.

Freeman K, Tsui P, Moore D, Emson PC, Vawter L, Naheed S, Lane P, Bawagan H, Herrity N, Murphy K, et al. (2001) Cloning, pharmacology, and tissue distribution of G-protein-coupled receptor GPR105 (KIAA0001) rodent orthologs. *Genomics* **78:**124–128.

Fricks IP, Maddileti S, Carter RL, Lazarowski ER, Nicholas RA, Jacobson KA, and Harden TK (2008) UDP is a competitive antagonist at the human $P2Y_{14}$ receptor. *J Pharmacol Exp Ther* **325:**588–594.

Fyfe M, Bergström M, Aspengren S, and Peterson A (2005) PAR-2 activation in intestinal epithelial cells potentiates interleukin-1beta-induced chemokine secretion via MAP kinase signaling pathways. *Cytokine* **31:**358–367.

Harden TK, Scheer AG, and Smith MM (1982) Differential modification of the interaction of cardiac muscarinic cholinergic and beta-adrenergic receptors with a guanine nucleotide binding component(s). *Mol Pharmacol* **21:**570–580.

Hauert AB, Martinelli S, Marone C, and Niggli V (2002) Differentiated HL-60 cells are a valid model system for the analysis of human neutrophil migration and chemotaxis. *Int J Biochem Cell Biol* **34:**838–854.

Huet E, Boulay F, Barral S, and Rabiet MJ (2007) The role of beta-arrestins in the formyl peptide receptor-like 1 internalization and signaling. *Cell Signal* **19:**1939–1948.

Johnson LG, Mewshaw JP, Ni H, Friedmann T, Boucher RC, and Olsen JC (1998) Effect of host modification and age on airway epithelial gene transfer mediated by a murine leukemia virus-derived vector. *J Virol* **72:**8861–8872.

Kam AY, Liu AM, and Wong YH (2007) Formyl peptide-receptor like-1 requires lipid raft and extracellular signal-regulated protein kinase to activate inhibitor-kappa B kinase in human U87 astrocytoma cells. *J Neurochem* **103:**1553–1566.

Klinker JF, Wenzel-Seifert K, and Seifert R (1996) G-protein-coupled receptors in HL-60 human leukemia cells. *Gen Pharmacol* **27:**33–54.

Kreda SM, Okada SF, van Heusden CA, O'Neal W, Gabriel S, Abdullah L, Davis CW, Boucher RC, and Lazarowski ER (2007) Coordinated release of nucleotides and mucin from human airway epithelial Calu-3 cells. *J Physiol* **584:**245–259.

Kreda SM, Seminario-Vidal L, Heusden C, and Lazarowski ER (2008) Thrombin-promoted release of UDP-glucose from human astrocytoma cells. *Br J Pharmacol* **153:**1528–1537.

Krzemiński P, Pomorski P, and Barañska J (2008) The $P2Y_{14}$ receptor activity in glioma C6 cells. *Eur J Pharmacol* **594:**49–54.

Lazarowski ER, Shea DA, Boucher RC, and Harden TK (2003) Release of cellular UDP-glucose as a potential extracellular signaling molecule. *Mol Pharmacol* **63:**1190–1197.

Lee BC, Cheng T, Adams GB, Attar EC, Miura N, Lee SB, Saito Y, Olszak I, Dombkowski D, Olson DP, et al. (2003) P2Y-like receptor, GPR105 ($P2Y_{14}$), identifies and mediates chemotaxis of bone-marrow hematopoietic stem cells. *Genes Dev* **17:**1592–1604.

Mahadeo DC, Janka-Junttila M, Smoot RL, Roselova P, and Parent CA (2007) A chemoattractant-mediated G_i-coupled pathway activates adenylyl cyclase in human neutrophils. *Mol Biol Cell* **18:**512–522.

Moore DJ, Murdock PR, Watson JM, Faull RL, Waldvogel HJ, Szekeres PG, Wilson S, Freeman KB, and Emson PC (2003) GPR105, a novel $G_i/_o$-coupled UDP-glucose receptor expressed on brain glia and peripheral immune cells, is regulated by immunologic challenge: possible role in neuroimmune function. *Brain Res Mol Brain Res* **118:**10–23.

Newburger PE, Chovaniec ME, Greenberger JS, and Cohen HJ (1979) Functional changes in human leukemic cell line HL-60: a model for myeloid differentiation. *J Cell Biol* **82:**315–322.

Paruch S, El-Benna J, Djerdjouri B, Marullo S, and Périanin A (2006) A role of p44/42 mitogen-activated protein kinases in formyl-peptide receptor-mediated phospholipase D activity and oxidant production. *FASEB J* **20:**142–144.

Rane MJ, Carrithers SL, Arthur JM, Klein JB, and McLeish KR (1997) Formyl peptide receptors are coupled to multiple mitogen-activated protein kinase cascades by distinct signal transduction pathways: role in activation of reduced nicotinamide adenine dinucleotide oxidase. *J Immunol* **159:**5070–5078.

Salomon Y, Londos C, and Rodbell M (1974) A highly sensitive adenylate cyclase assay. *Anal Biochem* **58:**541–548.

Schachter JB, Boyer JL, Li Q, Nicholas RA, and Harden TK (1997) Fidelity in functional coupling of the rat $P2Y_1$ receptor to phospholipase C. *Br J Pharmacol* **122:**1021–1024.

Scrivens M and Dickenson JM (2005) Functional expression of the $P2Y_{14}$ receptor in murine T-lymphocytes. *Br J Pharmacol* **146:**435–444.

Scrivens M and Dickenson JM (2006) Functional expression of the $P2Y_{14}$ receptor in human neutrophils. *Eur J Pharmacol* **543:**166–173.

Selvatici R, Falzarano S, Mollica A, and Spisani S (2006) Signal transduction pathways triggered by selective formylpeptide analogues in human neutrophils. *Eur J Pharmacol* **534:**1–11.

Servant G, Weiner OD, Herzmark P, Balla T, Sedat JW, and Bourne HR (2000) Polarization of chemoattractant receptor signaling during neutrophil chemotaxis. *Science* **287:**1037–1040.

Skelton L, Cooper M, Murphy M, and Platt A (2003) Human immature monocyte-derived dendritic cells express the G protein-coupled receptor GPR105 (KIAA0001, $P2Y_{14}$) and increase intracellular calcium in response to its agonist, uridine diphosphoglucose. *J Immunol* **171:**1941–1949.

Smith MM and Harden TK (1985) Muscarinic cholinergic receptor-mediated attenuation of adenylate cyclase activity in rat heart membranes. *J Cyclic Nucleotide Protein Phosphor Res* **10:**197–210.

Thomas EA, Matli JR, Hu JL, Carson MJ, and Sutcliffe JG (2000) Pertussis toxin treatment prevents 5-HT(5a) receptor-mediated inhibition of cyclic AMP accumulation in rat C6 glioma cells. *J Neurosci Res* **61:**75–81.

Wolff SC, Qi AD, Harden TK, and Nicholas RA (2005) Polarized expression of human P2Y receptors in epithelial cells from kidney, lung, and colon. *Am J Physiol Cell Physiol* **288:**C624–C632.

Address correspondence to: Dr. T. Kendall Harden, Department of Pharmacology, University of North Carolina, School of Medicine, Chapel Hill, NC 27599. E-mail: tkh@med.unc.edu

Downloaded from jpet.aspetjournals.org at ASPET Journals on January 20, 2018